Results for ANE

Roy Gross

The Unit of Nuclear Engineering, Ben-Gurion University of the Negev, Beer-Sheva 8410501, Israel

May 19, 2020

Action items

This document include discussions and results for publication in Annals of Nuclear Energy (ANE). So far, CMFD and pCMFD implemented and results were obtained. Comparing between CMFD and pCMFD, there's no difference at the convergence rate, and on the accuracy of the obtained results [1]. The global research question asked is **How does CMFD and pCMFD affect the Ronen method (RM), with its different parameters?**

Therefore, the following action items must be checked:

1. Convergence rate
    - Find cases in which CMFD does not converge, and pCMFD does
    - Study the effect of convergence parameters - modify No. of inner, outer and RM iterations.
2. Stability
    - Examining the **spectral radius -** ρ and performing numerical investigation of parameters (e.g. c, Δx). This is done by using the function *alter-c* by Tomatis.
3. Additional implementations - testing new numerical implementations
    - Direct change of the diffusion coefficient (line 912 within FD*) [2]
    - odCMFD (uncomment line 1007 within FD*) [3]

where

- ritmax, rtoll - RM parameters
- iitmax, itoll - inner iteration parameters
- oitmax, otoll - outer iteration parameters

The file of convergence data has three variables:

1. err - RM iterations error, size of [1,ritmax]
2. orr - outer iterations error, size of [oitmax, iitmax]

3. iitmax - inner iterations erros, size of [ritmax, oitmax, iitmax]

and this is the order of extracting the variables from the .npy file.

Iterations Effect

Ronen method iterations are set to max (very high number), and the simulation will stop when the RM iteration will converge or show unforeseen behavior. The thresholds are equal to $1e-6$, and the number of cells are $I = 100$. Both boundary conditions are set to void. the idea behind this test is to check under which combination of inner and outer iterations, the RM converge the faster.

Homogeneous case

The first test case is a homogeneous plane geometry [4]. The combinations between inner and outer iterations are shown in Table. 1. Two / three successive numbers in one cell, marks the number of cells $I = 50, 100, 150$.

Outer/Inner	1	2	5	10	20	50	100	150	200
1	393 (422)	387 (416)	(416)						(417)
2	387 (415)								(416)
5	(416)		(415)						
10	(416)			387 (415)	387 (415)	387	387	387	
20				387 (415)	387 (415)	387	387	387	
50				387 (415)	387 (415)	387	387	387	
100				387 (415)	387 (415)	387	387	387	
150				387 (415)	387 (415)	387	387	387	
200	(416)			387 (415)	387 (415)	387	387	387	

Table 1: Combination of inner and outer iterations for RM convergence test, homogeneous case. CMFD and (pCMFD).

Heterogeneous case

Heterogeneous case is by [5]. In order to keep Δ equal ($\Delta_w = \Delta_f$) between water and fuel regeion, the number of cells within the water are 5, and within the fuel media is 14, calculated by the simple relation ${}^{L_w}/_{I_w} = {}^{L_f}/_{I_f}$. The core under consideration is No.

3, which is the more heterogeneous between the three cores, shown at the reference. Results for different inner and outer iterations are shown in Table. 2. Some relations between I_w and I_f: 3-8, 4-11, 5-14, 8-22.

Outer/Inner	1	2	5	10	20	50	100	150	200
1	832 (840)	724	731	732			733		
2	719 (752)		728						
5	721 (754)			729					
10	722								
20									
50	723					730			
100									
150									
200	723								730 (763)

Table 2: Combination of inner and outer iterations for RM convergence test. CMFD and (pCMFD).

Threshold Effect

The effect of the inner and outer thresholds ($otoll$ and $itoll$) are examined here. The idea is to examine the effect of various combinations of tolerances on the Ronen method convergence, how fast, and if it converges at all. How far does the inner and outer iterations has to converge? In the above section, it was observed that the RM needs approximately 300 iterations to reach $rtoll \approx 10^{-5}$, and more 500 iterations to reach 10^-6. The results are shown in Tables. 3, 4. Outside the parenthesis, the results for the CMFD are shown, and inside the parenthesis, the results for the pCMFD. Regarding the heterogeneous case, the number of cells within the water is 3, and within fuel region is 8.

otoll/itoll	10^{-4}	10^{-5}	10^{-6}
10^{-4}	391 (419)	390 (419)	387 (417)
10^{-5}	389 (418)	389 (418)	387 (417)
10^{-6}	387 (415)	388 (415)	387 (415)

Table 3: Combination of inner and outer thresholds, and the effect on the number of RM iterations until convergence. Homogeneous case. CMFD, (pCMFD)

otoll/itoll	10^{-4}	10^{-5}	10^{-6}
10^{-4}	734 (767)	734 (767)	733 (766)
10^{-5}	733 (766)	733 (766)	733 (766)
10^{-6}	730 (763)	730	730 (763)

Table 4: Combination of inner and outer thresholds, and the effect on the number of RM iterations until convergence. Heterogeneous case, core No. 3 [5]. CMFD, (pCMFD)

Scattering Ratio Effect

Homogeneous Case

One of the limitations of diffusion, is that absorption is small compared to scattering (poorly absorbing medium). The scattering ratio c is the ratio between the scattering cross section, and absorption cross section. Challenging the diffusion calculation and the Ronen method, by changing the scattering ratio (Denoted by c). This test is performed on the homogeneous plane geometry.

The cross section updates goes as follows:

1. STEP 1: choose c_g^{new}
2. STEP 2: calculate $\sigma_{s,0,g}^{\text{old}} = \sum_{g'=1}^{G} \sigma_{s,0,g' \leftarrow g}^{\text{old}}$, by anonymous function *sd*.
3. STEP 3: calculate new scattering cross section $\sigma_{s,0,g' \leftarrow g}^{\text{new}}$ by Eq.1, 2.
4. STEP 4: calculate new absorption cross section $\sigma_{a,g}^{\text{new}}$, by Eq. 3.
5. STEP 5: calculate new fission cross section $\nu\sigma_{f,g}^{\text{new}}$, by Eq. 4.

Total cross section, $\sigma_{t,g}$ remains the same as of original value. The modified values of the cross sections are shown in Table. 5, and the effect of the scattering ratio c on them, shown in Fig. 1

$$\frac{\sigma_{s,0,g' \leftarrow g}^{\text{new}}}{c_g^{\text{new}}} = \frac{\sigma_{s,0,g' \leftarrow g}^{\text{old}}}{c_g^{\text{old}}} \ , \tag{1}$$

where

$$c_g^{\text{old}} = \frac{\sigma_{s,0,g}^{\text{old}}}{\sigma_{t,g}} \ . \tag{2}$$

$$\sigma_{a,g}^{\text{new}} = \sigma_{t,g} - \sigma_{s,0,g}^{\text{new}} \ . \tag{3}$$

$$\frac{\nu\sigma_{f,g}^{\text{new}}}{\sigma_{a,g}^{\text{new}}} = \frac{\nu\sigma_{f,g}^{\text{old}}}{\sigma_{a,g}^{\text{old}}} \tag{4}$$

$$\nu\sigma_{f,g}^{\text{new}} = \nu\sigma_{f,g}^{\text{old}} \frac{\sigma_{a,g}^{\text{new}}}{\sigma_{a,g}^{\text{old}}} \ . \tag{5}$$

Test	A	B	C	D-ref	E	F	G
c_1	0.7	0.8	0.9	0.98081	0.99	0.999	1.0
c_2	0.7	0.8	0.9	0.91757	0.99	0.999	1.0
$\sigma_{s,0,g}^{\text{new}}$	0.3718	0.42492	0.47803	0.52096	0.52584	0.53062	0.53115
	0.91041	1.04046	1.17052	1.19338	1.28757	1.29928	1.30058
$\sigma_{a,g}^{\text{new}}$	0.15935	0.10623	0.05312	0.01019	0.00531	0.00053	1.11022e-16
	0.39017	0.26012	0.13006	0.1072	0.01301	0.0013	0.0
$\nu\sigma_{f,g}^{\text{new}}$	0.11193	0.07462	0.03731	0.00716	0.00373	0.00037	1.11022e-16
	0.51422	0.34282	0.17141	0.14128	0.01714	0.00171	0.0
k_{eff}	0.699968	0.705574	0.71456	0.743445	0.578707	0.15831	3.53805e-15

Table 5: Modified cross sections, and k_{eff}, for each scattering ratio c_g^{new}. $\epsilon_{\text{RM}} = 10e-5$

The reference homogeneous case [4] has scattering ratio of $c_1 = 0.98081, c_2 = 0.91757$, for total cross section of $\sigma_{t,1} = 0.53115, \sigma_{t,2} = 1.30058$. The scattering ratio of the fast group is larger than of the thermal group, due to the fact that scattering reaction is larger for fast neutrons than thermal group. The cases are tested shown in Table **??**. Scattering ratio larger than 1, resulting in negative cross section, which is not physical.

The vertical dashed lines in Fig. 1 represent the reference case (D, in Table. 5. Lower scattering ratio, increasing the absorption and fission cross sections,which should've increase the multiplication factor, but on the other hand, this decreases the scattering cross section, which resulting in less neutrons scatter from the fast group to the thermal group. Increasing the scattering ratio, yields in larger scattering cross section. Therefore, absorption cross section decreases, as a result, fission cross section decrease as well. At a value close to 1.0, $\nu\sigma_{f,2}$ is very low, close to zero, and the multiplication factor k_{eff} equal to zero. In other words, no fission occur in the system, from

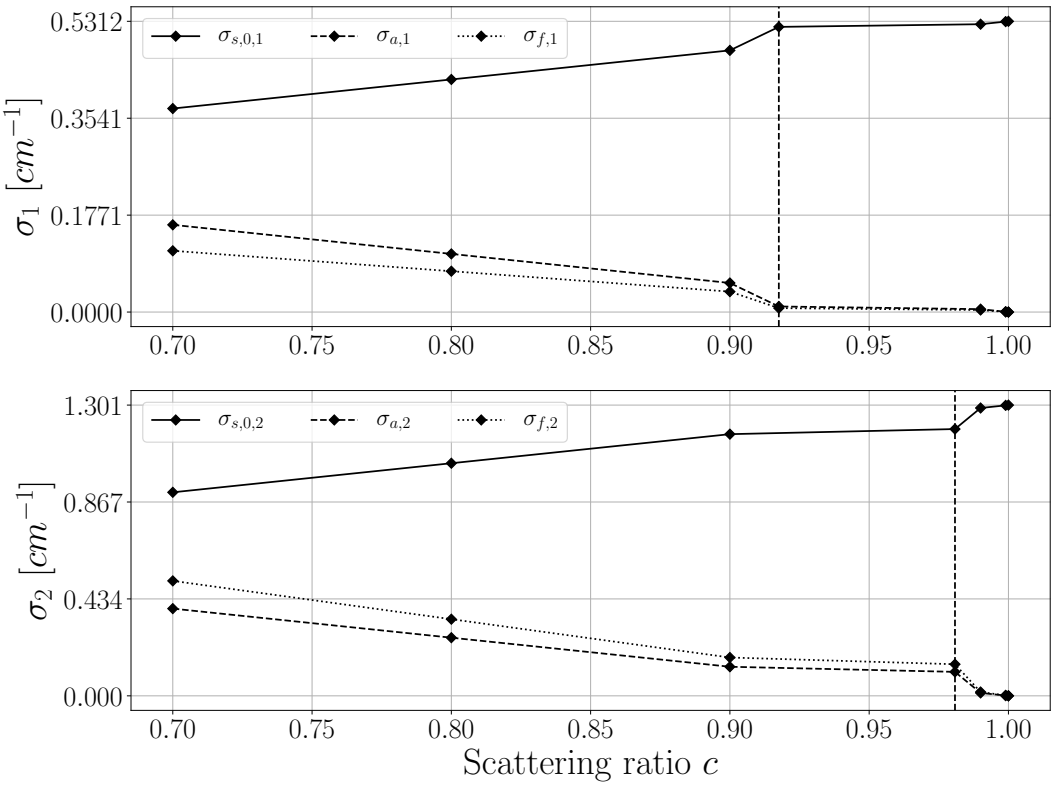

Figure 1: Effect of scattering ratio, on the macroscopic cross secions.

thermal neutrons. This decline in the values of absorption and fission cross sections are observed for values of c_g larger than the reference case. When $c = 1.0$, the scattering cross section is equal to the total cross section $\sigma_{t,g}$ (From Eq. 3), meaning that there's no absorption within the system, and no fission occur.

Heterogeneous case

A symmetrical, one-dimensional geometry composed of three adjacent planes, were created, shown in Fig. 2. Denoting the regions as L, C and R, which stands for Left, Center and Right, respectively. The left and right regions has the same properties, i.e., cross sections [4] and width, equal to at least 5-6 mean free paths λ_g. Center region, is the one that has different parameters. Cross sections of the center region are modified, by changing the scattering ratio c_g, according to Eqs. 2- 4. Furthermore, the width of the latter region will be modified, in order to examine the effect on the whole domain. This test is done in order to study the following:

1. The interaction of such structure, focuse on the performances of RM near the boundaries.

2. Challenge the RM, study the convergence property of CMFD.

3. Compare the results of Diffusion, RM and discrete ordinate S_N.

Scattering ratio, width and cross sections, are shown in Table. 6.

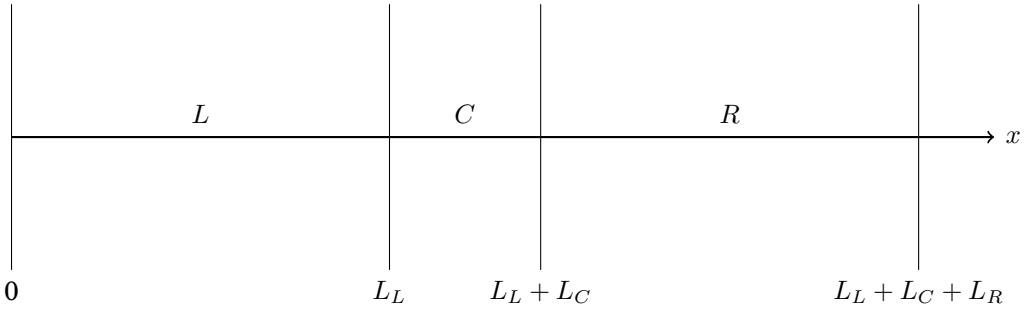

Figure 2: Three-regions symmetrical domain.

Test/Params	1	2	3	4-ref	5	6
c_g	0.1	0.5	0.8	0.98081	0.99	0.999
	0.1	0.5	0.8	0.91757	0.99	0.999
$\sigma^{\text{new}}_{s,0,g' \leftarrow g}$	0.05312	0.26557	0.42492	0.52096	0.52584	0.53062
	0.13006	0.65029	1.04046	1.19337	1.28757	1.29928
$\sigma^{\text{new}}_{a,g}$	0.47803	0.26558	0.10623	0.01019	0.00531	0.00053
	1.17052	0.65029	0.26012	0.10721	0.01301	0.0013
$\nu\sigma^{\text{new}}_{f,g}$	0.3358	0.18656	0.07462	0.00716	0.00373	0.00037
	1.54267	0.85704	0.34282	0.14129	0.01714	0.00171

Table 6: Heterogeneous test cases parameters, of the center region. First parameter is of the fast group, the lower of the thermal group.

Spectral Radius

A parameter which allows to check the stability of the numerical scheme, is the **spectral radius**. The spectral radius represents the convergence property of the finite difference calculation used in the nonlinear acceleration [6], [7]. The spectral radius evaluated by Eq. 6, in case of CMFD implementation.

$$\rho = \frac{\left\| \delta D^{(n)} - \delta D^{(n-1)} \right\|_2}{\left\| \delta D^{(n-1)} - \delta D^{(n-2)} \right\|_2} \quad . \tag{6}$$

$$\|x\|_2 = \left(\sum_{g'=1}^{G} \sum_{i=0}^{I-1} \delta D_{g,i} \right)^{1/2} \quad . \tag{7}$$

where n stand for iteration index, and i for cell index. The nominator and denominator are the second norm of the difference between two consecutive iterations, which is simply the distance between two points. Analytical form of the second norm is shown in Eq. 7. The spectral radius obtained after the inner and outer iterations are converged.

Numerical code:

1. Step 1: calculate the difference between two consecutive Ronen iterations. This is possible starting from the second iteration (See Eq. 6).
2. Step 2: calculate the separately the nominator and denominator of Eq. 6, using *numpy.linalg.norm*.

   https://numpy.org/doc/1.18/reference/generated/numpy.linalg.norm.html
3. Step 3: divide both terms, resulting in spectral radius ρ.

The effect of cell size Δ on the spectral radius

CMFD is stable for this coarse cells, but unstable for optically thick coarse cells [8]. On the other hand, pCMFD is stable for optically thick coarse cells. The affect of Δ on the spectral radius, for difference cell points, is shown in Table. 7, and the change of the spectral radius of converged Ronen iteration, for difference cell sizes, presented in Fig. 3. The width of the one-dimensional plane is $L = 21.5[cm]$ [4].

The spectral radius decreases, as the number of node decreases (or as the size of cell's width increases). Due to error in my current version of the code (FD*), there's big gap between $2 < I < 10$, or between $3.5833 < \Delta < 10.75$.

Case/Params	A	B	C	D	E	F	G
I	1	2	5	10	50	100	150
Δ[CM]	21.5	10.75	4.3	2.15	0.43	0.215	0.14333
$\rho^{(N)}$	0.04311	0.04294		0.41994	0.95397	0.98649	0.99301
rit-cvg	4	4		12	84	207	312

Case/Params	H	I	K
I	200	300	400
Δ[CM]	0.1075	0.071667	0.05375
$\rho^{(N)}$	0.99547	0.99729	0.99793
rit-cvg	410	557	655

Table 7: Test cases for examine the effect of mesh size on the spectral radius.$\epsilon_{\text{RM}} = 10e-5$

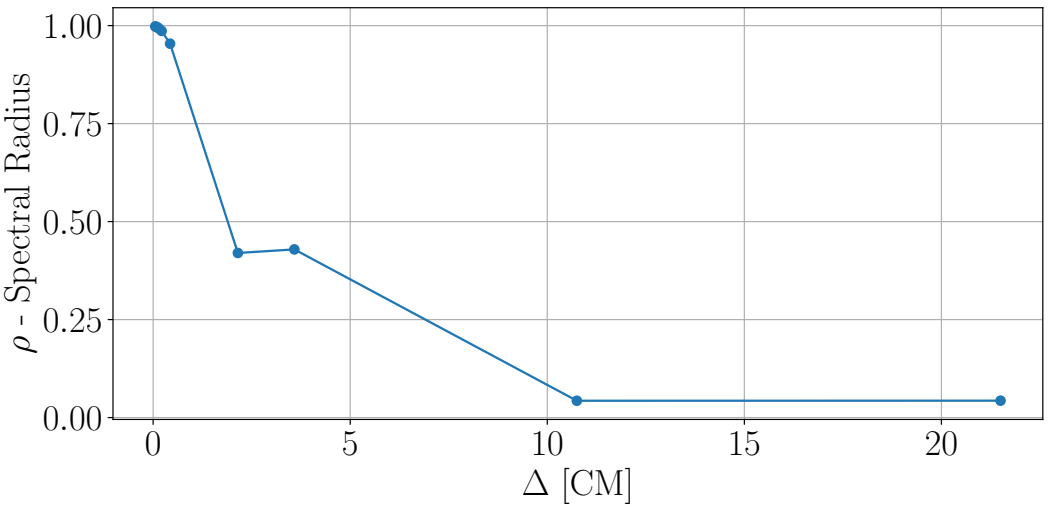

Figure 3: Effect of cell width Δ, on the Spectral radius ρ.

Bibliography

[1] R. Gross, D. Tomatis, and E. Gilad. High-accuracy neutron diffusion calculations based on integral transport theory. *The European Physical Journal - Plus (EPJ Plus)*, 2020. Submitted.

[2] Yigal Ronen. Accurate relations between the neutron current densities and the neutron fluxes. *Nuclear Science and Engineering*, 146(2):245–247, 2004.

[3] Ang Zhu, Michael Jarrett, Yunlin Xu, Brendan Kochunas, Edward Larsen, and Thomas Downar. An optimally diffusive coarse mesh finite difference method to accelerate neutron transport calculations. *Annals of Nuclear Energy*, 95:116–124, 2016.

[4] D. Tomatis and A. Dall'Osso. Application of a numerical transport correction in diffusion calculations. In *International Conference on Mathematics and Computational Methods Applied to Nuclear Science and Engineering (M&C 2011), Rio de Janeiro, RJ, Brazil, May 8-12, 2011*, 05 2011.

[5] F. Rahnema and E. M. Nichita. Leakage corrected spatial (assembly) homogenization technique. *Annals of Nuclear Energy*, 24(6):477–488, 1997.

[6] Yamamoto. Convergence property of responce matrix method for various finite-difference formulation usedin the nonlinear acceleration method. *Nuclear Science and Engineering*, 149:259–269, 2005.

[7] Yongjin Jeong, Jinsu Park, Hyun Chul Lee, and Deokjung Lee. Convergence analysis of two-node cmfd method for two-group neutron diffusion eigenvalue problem. *Journal of Computational Physics*, 302, 12 2015.

[8] M. Jarrett, B. Kochunas, A. Zhu, and T. Downar. Analysis of stabilization techniques for CMFD acceleration of neutron transport problems. *Nuclear Science and Engineering*, 184(2):208–227, 2016.